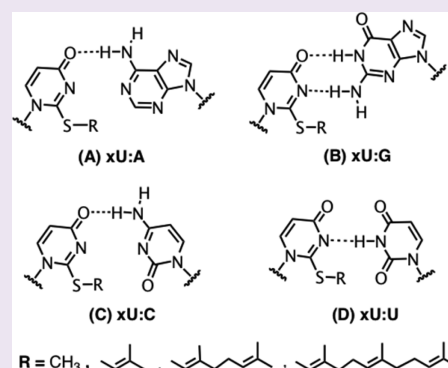


Nature's Selection of Geranyl Group as a tRNA Modification: The Effects of Chain Length on Base-Pairing Specificity

Phensinee Haruehanroengra,^{†,‡,§,¶} Sweta Vangaveti,^{‡,§} Srivathsan V. Ranganathan,[‡] Rui Wang,^{†,‡} Alan Chen,^{†,‡,¶} and Jia Sheng^{*,†,‡,¶}[†]Department of Chemistry and [‡]The RNA Institute, University at Albany, State University of New York, 1400 Washington Avenue, Albany, New York 12222, United States

Supporting Information

ABSTRACT: The recently discovered geranyl modification on the 2-thio position of wobble U34 residues in tRNA^{Glu}, tRNA^{Lys}, and tRNA^{Gln} in several bacteria has been found to enhance the U:G pairing specificity and reduce the frameshifting error during translation. It is a fundamentally interesting question why nature chose a C10 terpene group in tRNA systems. In this study, we explore the significance of the terpene length on base-pairing stability and specificity using a series of 2-thiouridine analogues containing different lengths of carbon chains, namely, methyl- (C1), dimethylallyl- (C5), and farnesyl-modified (C15) 2-thiothymidines in a DNA duplex. Our thermal denaturation studies indicate that the relatively long chain length of \geq C10 is required to maintain the base-pairing discrimination of thymidine between G and A. The results from our molecular dynamics simulations show that in the T:G-pair-containing duplex, the geranyl and farnesyl groups fit into the minor groove and stabilize the overall duplex stability. This effect cannot be achieved by the shorter carbon chains such as methyl and dimethylallyl groups. For a duplex containing a T:A pair, the terpene groups disrupt both hydrogen bonding and stacking interactions by pushing the opposite A out of the helical structure. Overall, as the terpene chain length increases, the xT:G pair stabilizes the duplex, whereas the xT:A pair causes destabilization, indicating the evolutionary significance of the long terpene group on base-pairing specificity and codon recognition.



INTRODUCTION

It is well-known that natural RNAs from all domains of life are heavily modified with over 140 chemical functionalities.^{1,2} These modifications play critical roles in gene regulation and many human diseases by different mechanisms such as tuning RNA structures, recruiting specific proteins that are involved in other metabolic pathways, and affecting translational fidelity and efficiency with different ribosomal interactions.^{3–7} In addition, their cellular levels and distributions can be dynamically changed in response to stress such as nutrient deprivation and heat shock.^{8,9} It has recently been shown that some of these processes are reversible and the dynamic modification levels can affect translation initiation as well as overall gene expression efficiency.¹⁰ Furthermore, many of these post-transcriptional modifications are hypothesized to be chemical fossils from the early RNA world, where the structural and functional diversity of RNA may have been further enhanced by these moieties prior to the emergence of proteins.¹¹

Among all RNA species, tRNAs contain the greatest number of modifications, which, depending on the location, can influence tRNA folding, stability, amino acids charging, as well as codon recognition and decoding.^{12–20} Particularly, the wobble (first anticodon) position 34 in the anticodon loop of a tRNA exhibits a wide variety of modifications that are directly

involved in the anticodon–codon interactions and translation regulation.^{21,22} The wobble uridine is often thiolated to form 2-thiouridine (s^2U) through the Iscs-MnmA pathway.²³ The 2-thiolation of U34 is of particular importance in ribosomal binding and wobble base pairing of specific tRNAs such as tRNA^{Lys}_{UUU}^{24,25} and tRNA^{Glu}_{UUC}.²⁶ The s^2U can be further modified by the 5-methylaminomethyl (5-mnm)- or 5-carboxymethylaminomethyl (5-cmnm)-groups on position 5 of the pyrimidine ring to form mnm⁵ s^2U or cmnm⁵ s^2U through the MnmEG pathways (compounds 3 and 4 in Figure 1).²³ These two groups are also found to be important for efficient codon recognition.^{26,27}

The sulfur atom in s^2U can be further replaced with selenium to form 2-selenouridine (se^2U) by the selenouridine synthase SelU (also referred to as MnmH) in the presence of selenophosphate (Figure 2a).²⁸ Very recently, SelU has also been shown to use geranyl pyrophosphate as the cofactor to generate geranylated 2-thiouridine (ges^2U) (compound 5 in Figure 1 and Figure 2b) in tRNAs specific for lysine (tRNA^{Lys}_{UUU}), glutamine (tRNA^{Gln}_{UUG}), and glutamic acid (tRNA^{Glu}_{UUC}).^{29,30} It is estimated that approximately 2.8–6.7%

Received: February 7, 2017

Accepted: April 5, 2017

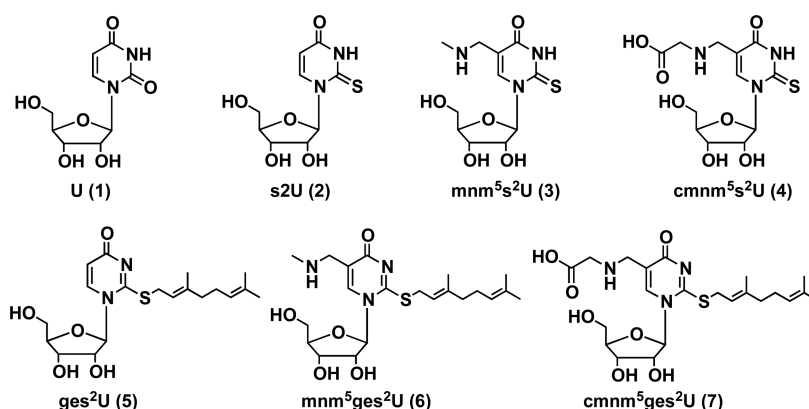


Figure 1. Chemical structures of uridine (U, 1), 2-thiouridine (s^2U , 2), 5-methylaminomethyl-2-thiouridine (mnm^5s^2U , 3), 5-carboxymethylaminomethyl-2-thiouridine ($cmnm^5s^2U$, 4), geranylated 2-thiouridine (ges^2U , 5), 5-methylaminomethyl-S-geranyl-2-thiouridine (mnm^5ges^2U , 6), and 5-carboxymethylaminomethyl-S-geranyl-2-thiouridine ($cmnm^5ges^2U$, 7).

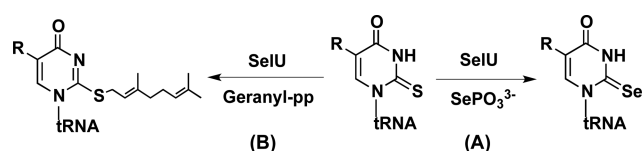


Figure 2. Selenouridine synthase (SelU) has a dual function: (A) to replace sulfur with selenium in the presence of selenophosphate; and (B) to install a geranyl group to the sulfur atom in the presence of geranyl pyrophosphate. The R group represents the mnm^5 - or $cmnm^5$ - in position 5.

of these three tRNAs are modified by this unique lipid group (up to ~ 400 geranylated nucleotides per cell) in several bacteria including *E. coli*, *E. aerogenes*, *P. aeruginosa*, and *S. typhimurium*.²⁹ Similarly, ges^2U can be further modified to 5-methylaminomethyl-S-geranyl-2-thiouridine (mnm^5ges^2U) or 5-carboxymethylaminomethyl-S-geranyl-2-thiouridine ($cmnm^5ges^2U$) (compounds 6 and 7 in Figure 1).

It has been observed that this highly hydrophobic geranyl group increases the codon recognition efficiency of $tRNA^{Glu}_{UUC}$ to GAG over GAA and decreases the frameshifting errors during translation.²⁹ In prior work, we have directly measured stronger base-pairing specificity between ges^2U and G over A in the context of canonical duplexes,^{31,32} consistent with the findings of Sierant et al.³³ Examination of the potential base-pairing patterns (Figure 3) suggests that a consequence of the geranyl functionality is to switch the N3 of uridine from a

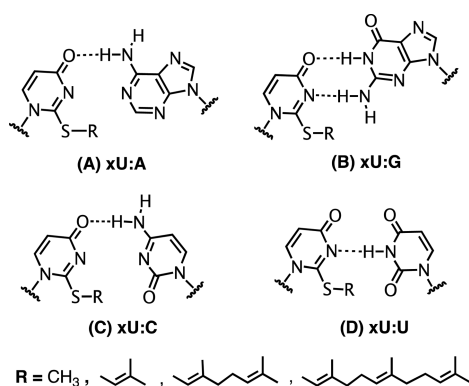
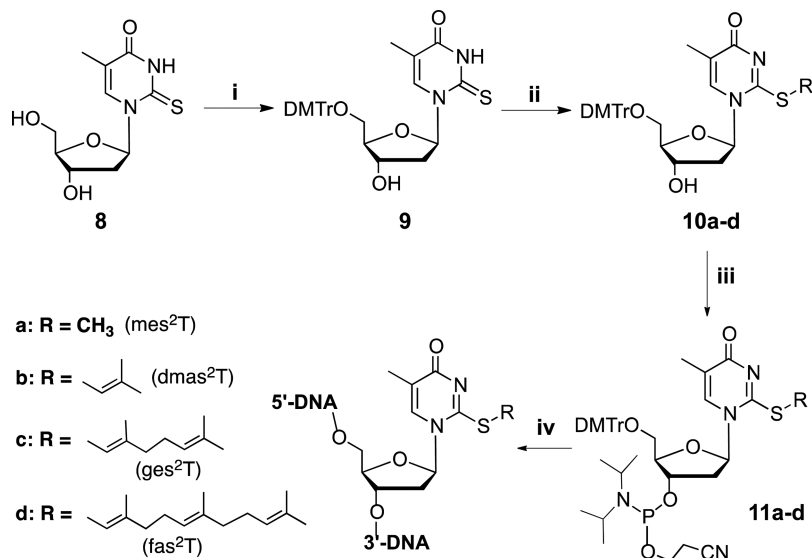


Figure 3. Proposed base-pairing patterns between the geranyl-2-thiouridine analogues (xU) with different length of carbon chains and A, G, C, U, respectively.

hydrogen bond donor to a hydrogen bond acceptor. As demonstrated by our previous molecular simulation studies, only guanosine (G) with two consecutive hydrogen bonding donors can form two relatively stable hydrogen bonds with the modified uridine, whereas the base pairing with the other three partners (i.e., A, C, and U) is not as stable, exhibiting only a single, easily broken hydrogen bond.^{31,32} Given this hydrogen bonding pattern and the fact that each of the two codons for glutamic acid, lysine, and glutamine ends in either A or G, it is very likely that the geranylated uridine will promote base pairing with the G-ending codon while restricting pairing with the A-ending ones for each of these amino acids.

However, a closer look at the base-pairing patterns in Figure 3 reveals that even a small methyl group on sulfur might still maintain the same pairing patterns as seen with the geranyl group. In addition, although there are many natural terpene groups with different lengths and shapes of carbon chains available in live cells as geranyl analogues and as building blocks for lipid biosynthesis,^{34,35} no such lipid-nucleosides have been discovered. From this aspect, it is an intriguing question why nature selected the geranyl group over other terpene analogues in modifying the tRNA wobble uridine. Although it has been speculated that the geranylated 2-thiouridine might be the intermediate compound during the selenation of 2-thiouridine,^{36,37} the same argument also applies here because a small methyl group could have been used to activate the sulfur center for selenium replacement.^{38,39} Overall, the appearance of this hydrophobic C10 geranyl group in tRNA might represent an evolutionary advantage. From the evolutionary point of view, because many RNA chemical modifications have been regarded as relic components of the RNA world, the lipid modifications in RNA could be linked to ancient RNA-mediated lipid synthesis, where these RNA-lipid conjugations might have played critical roles in many prebiotic chemical processes during the early stages of life.⁴⁰

Towards the exploration and utilization of nature's selection of geranyl modification in tRNA, in this work, we synthesized a series of geranyl 2-thiouridine analogues including methyl-(C1), dimethylallyl- (C5), and farnesyl-2-thiouridines (C15) and DNA oligonucleotides containing these modifications to investigate the significance of carbon chain length on base-pairing stability and specificity. Our thermal denaturation studies indicate that the relatively long chain length of $\geq C10$ is required to maintain the base-pairing discrimination between G and A, which is unexpected from the base-pairing pattern

Scheme 1. Synthesis of DNA Oligonucleotides Containing *S*-Geranyl-2-thiothymidine Analogues (xT)^a

^a(i) Dimethoxytrityl chloride (DMTrCl), pyridine, room temperature, 85%. (ii) a. Methyl iodine, *N,N*-diisopropylethylamine (DIEA), MeOH, room temperature; b. dimethylallyl bromide, DIEA, MeOH, room temperature; c. geranyl bromide, DIEA, MeOH, room temperature; d. farnesyl bromide, DIEA, MeOH, room temperature. The overall yields of these reactions are above 90%. (iii) 2-Cyanoethyl *N,N*-diisopropylchlorophosphoramidite, *N,N*-diisopropylethylamine (DIEA), CH₂Cl₂, room temperature. Yields ~80%.

shown in Figure 3. Our molecular dynamics studies show that in duplexes containing T:G pairs, both geranyl and farnesyl groups fit into the minor groove and improve the overall duplex stability. This effect cannot be achieved by the shorter carbon chains such as the methyl and dimethylallyl groups. However, in the T:A-pair-containing duplex, the terpene groups widen the local helical diameter and disrupt the hydrogen bond formation. Overall, as the terpene chain length increases, the xT:G pair stabilizes the duplex, whereas the xT:A pair causes destabilization.

RESULTS AND DISCUSSION

Synthesis of Geranyl-2-thiothymidine Analogues and Their Containing Oligonucleotides. As shown in Scheme 1, we started the synthesis from 2-thiothymidine by the selective tritylation of its 5'-hydroxyl group. The terpene functional analogues including methyl-, dimethylallyl-, geranyl-, and farnesyl-groups were subsequently added to the 2-thio position to generate the key intermediates 10a–d in high yields, followed by the construction of the final xT phosphoramidite building blocks 11a–d for the oligonucleotide solid-phase synthesis. It has been demonstrated that the geranyl group is compatible with the standard reagents and conditions of solid-phase synthesis using dichloromethane as the solvent.³¹ Consistently, all these geranyl analogues are also stable during the oligonucleotide synthesis with iodine and acidic treatments, cleavage with basic ammonium aqueous solution, and HPLC purification processes. The purified oligonucleotides were confirmed by mass-spectrometry analysis (Table S1).

Thermal Denaturation and Base-Pairing Studies of xT-Containing Duplexes. The successful synthesis of these modified oligonucleotides enabled the direct measurement of the base-pairing stability and specificity effects of these geranyl-thymidine derivatives (xT) through thermal denaturation experiments using the same 11mer-duplex sequence as used in our earlier study of the geranyl group,³² [5'-CTTCTxTGTCCG-3' and 5'-CGGACYAGAAG-3'], with

the Watson–Crick and other noncanonical mismatched base pairs (xT pairs with Y) shown in Figure 4. The UV-melting temperature (T_m) curves of native and modified duplexes and the corresponding melting data are shown in Figure 5 and Table 1.

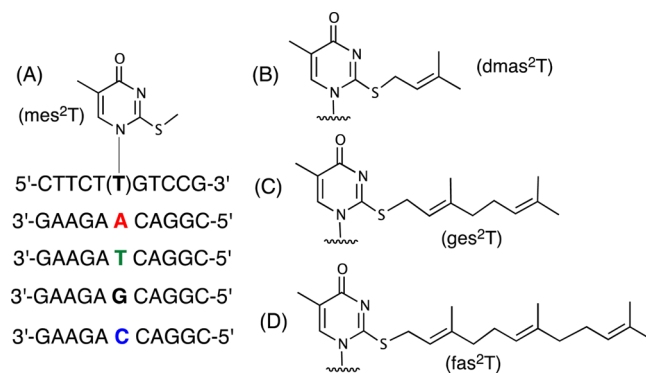


Figure 4. Modified DNA strand containing *S*-geranyl-2-thiothymidine derivatives xT including methyl- (A), dimethylallyl- (B), geranyl- (C), and farnesyl-2-thiothymidine (D).

All the different lengths of terpene chains on 2-thiothymidine reduce the overall base-pairing stability when compared to native thymidine. In particular, the canonical Watson–Crick base-pairing stability (xT:A) is dramatically reduced after the modifications (entry 1 in Table 1). The melting temperatures (T_m) of DNA duplexes containing methyl-2-thiothymidine (mes²T), dimethylallyl-2-thiothymidine (dmas²T), geranyl-2-thiothymidine (ges²T), and farnesyl-2-thiothymidine (fas²T) are reduced by 13.0 °C, 13.9 °C, 16.0 °C, and 19.4 °C, respectively, corresponding to an increased ΔG^0 of 4.6, 4.7, 4.3, and 5.2 kcal/mol when compared to the native T:A-pair-containing duplex, indicating the increasing instability of the T:A pair with the increase in length of the carbon chain. However, in the duplexes containing other noncanonical base

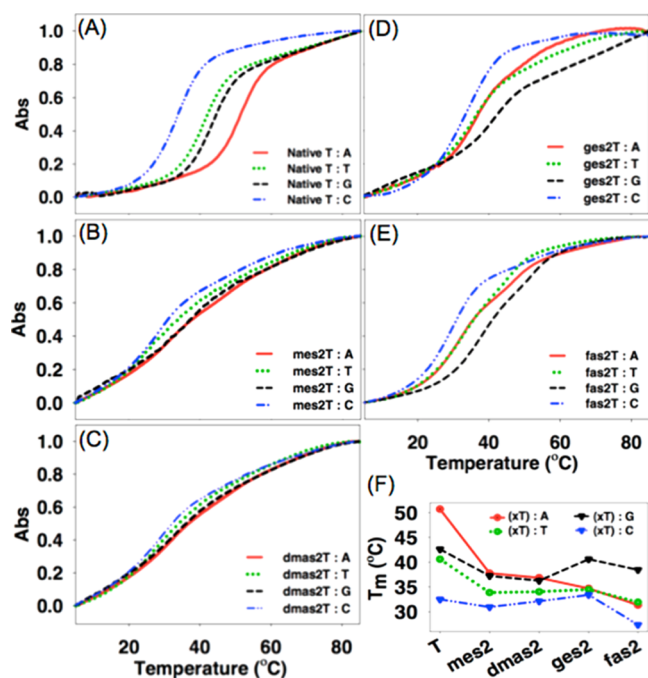


Figure 5. Normalized UV-melting curves of DNA duplexes, 5'-CTTCT(xT)GTCCG-3' and 3'-GAAGA Y CAGGC-5' where (xT) base pairs with Y. The (xT) represents (A) native thymidine, (B) *S*-methyl-2-thiothymidine, (C) *S*-dimethylallyl-2-thiothymidine, (D) *S*-geranyl-2-thiothymidine, and (E) *S*-farnesyl-2-thiothymidine. (F) Summary of melting temperatures (T_m) of DNA duplexes with various base pairs versus different xT.

pairs, these modified residues show much less structural perturbation. The T_m s of duplexes containing xT:T pairs decrease by 6.8, 6.6, 6.1, and 8.7 °C (entry 2) and the ones containing a xT:G pair decrease by 5.4, 6.3, 2.0, and 4.2 °C (entry 3). Similarly, the xT:C-pair-containing duplexes show a slight T_m decrease by 1.6 °C for mes²T and 0.4 °C for dmas²T. Although a slight T_m increase by 0.9 °C was observed for the ges²T:C mismatched duplex, the fas²T:C-pair-containing duplex shows a relatively bigger T_m decrease by 5.1 °C (entry 4). Interestingly, for each of the three mismatch paired duplexes, the overall thermal stability reaches the maximum when the carbon chains grow longer from 1 to 10 and drops again at C15 with the farnesyl group.

When directly comparing the duplex T_m s of each modification in xT:A with the other three mismatched pairs (as shown in the ΔT_m columns of Table 1), consistent with the native thymidine, both mes²T and dmas²T decrease the duplex stability when they pair with T, G, and C; however, the xT:G-containing duplexes show very slight T_m drop (only by 0.5 °C). In contrast, both geranyl and farnesyl groups dramatically enhance the overall stability of xT:G-containing duplex over other mismatched ones with the T_m of ges²T:G duplex 5.9 °C higher than the ges²T:A duplex, and the one with farnesyl group is 7.1 °C higher than the fas²T:A counterpart. Because the native T:G-pair-containing duplex is less stable when compared to the normal T:A pair duplex (-8.1 °C), the data collectively indicate that both geranyl and farnesyl groups can improve the base-pairing ability of T:G pair compared to the T:A and other mismatched pairs, whereas the methyl and dimethylallyl groups with short carbon chains cannot achieve this base-pairing discrimination, as illustrated in Figure 5F.

Table 1. DNA Duplex Stability and Base-Pairing Specificity of Methyl-2-thiothymidine (mes²T), Dimethylallyl-2-thiothymidine (dmas²T), Geranyl-2-thiothymidine (ges²T), and Farnesyl-2-thiothymidine (fas²T) in the Context of a 11-Mer DNA Duplex [5'-CTTCT(xT)GTCCG-3' and 3'-GAAGA Y CAGGC-5']

entry, pair	T			mes ² T			dmas ² T			ges ² T			fas ² T		
	T_m^a (°C)	ΔT_m^b (°C)	$-\Delta G^{0c}$ (kcal/mol)	T_m (°C)	ΔT_m (°C)	$-\Delta G^0$ (kcal/mol)	T_m (°C)	ΔT_m (°C)	$-\Delta G^0$ (kcal/mol)	T_m (°C)	ΔT_m (°C)	$-\Delta G^0$ (kcal/mol)	T_m (°C)	ΔT_m (°C)	$-\Delta G^0$ (kcal/mol)
1 xT:A	50.7		12.3	37.7	36.8	7.7	34.7	34.7	8.0	31.3	31.3	7.1	31.3	31.3	7.1
2 xT:T	40.6	-10.1	8.7	33.8	-3.9	6.9	34.5	-0.2	7.8	31.9	0.6	7.2	31.9	0.6	7.2
3 xT:G	42.6	-8.1	9.6	37.2	-0.5	8.5	40.6	5.9	9.3	38.4	7.1	7.8	38.4	7.1	7.8
4 xT:C	32.5	-18.2	7.2	30.9	-6.8	6.4	33.4	-1.3	7.6	27.4	-3.9	6.0	27.4	-3.9	6.0

^aThe T_m were measured in sodium phosphate (10 mM, pH 6.5) buffer containing 100 mM NaCl. ^b ΔT_m values are relative to the duplex with U:A pair and xU:A pair, respectively. ^cObtained by nonlinear curve fitting using Meltwin 3.5.

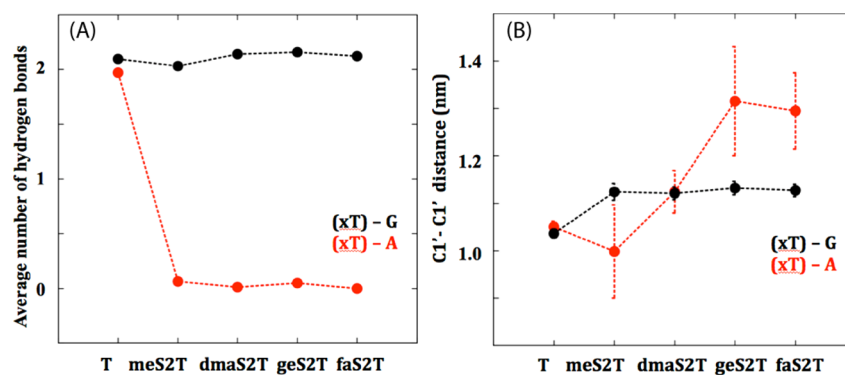


Figure 6. (A) Number of hydrogen bonds. (B) C1'–C1' distance calculated for the modified nucleotide (T, meS2T, dmaS2T, geS2T, and fas2T) and its complementary nucleotide A (red) and G (black).

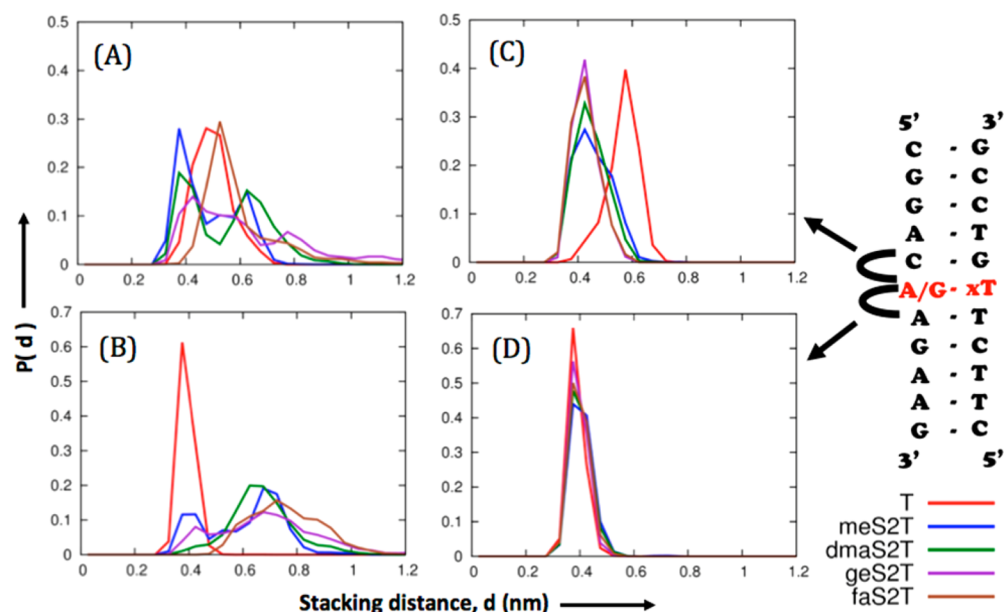


Figure 7. Probability of stacking distances (nm) between the xT paired A or G and their neighboring bases. (A) A with its 5'-C; (B) A with its 3'-A; (C) G with its 5'-C; and (D) G with its 3'-A. The distances are calculated between the centers of mass of the respective nucleobases.

It has been known that the 2-thiothymidine (S^2T) decreases the thermal stability of S^2T :G containing duplex by over 12 °C compared to the S^2T :A containing duplex in a 12mer DNA duplex context with similar sequences.⁴¹ The attachment of carbon chains with different length on the 2-thio position can gradually change the base-pairing patterns, especially between T:A and T:G pairs. This capacity of the 2-thio modification in pyrimidines might represent one of the evolutionary advantages for the natural 2-thiouridine derivatives in tRNA to selectively recognize, distinguish, and fine-tune the anticodon interactions with A-ending and G-ending codons. Specifically, the replacement of native uridine with 2-thiouridine analogues including 2-selenouridines^{38,39} at wobble position increases the recognition of A-ending codons. However, the alkylation of 2-thio position with short carbon chains such as methyl and dimethylallyl groups removes base-pairing specificity, and the incorporation of longer carbon chains like geranyl and farnesyl groups completely reverses the codon selectivity. This might also imply an adaptive strategy of tRNA to regulate the expression of certain proteins according to specific environmental conditions. The further selection between geranyl and farnesyl groups or other long terpene derivatives might be

based on the availability of each of the building blocks and the feasibility of the evolution of enzymes that can recognize and incorporate these modifications into tRNAs.

Structural Studies of xT-Containing Duplexes through Molecular Simulation. To further understand the structural basis for the additional stability that the geranyl and farnesyl groups impart to the xT:G containing duplex over other lengths of modifications, all-atom molecular dynamics (MD) simulation studies were performed. The modified DNA duplex [5'-CTTCT(xT)GTCCG-3' and 3'-GAAGA(A/G)-CAGGC-5'] was simulated with different modifications, where "xT" represents meS²T, dmaS²T, geS²T, or fas²T. Consistent with the hydrogen bonding patterns in Figure 3 as well as our previous simulation results,³² it is observed that there are two stable hydrogen bonds formed by the xT:G pair in all cases, whereas no stable hydrogen bond could be formed between xT and A for any of the modifications (Figure 6A). However, despite the hypothesized common hydrogen bonding pattern of xT:G and xT:A pairing over the different lengths of carbon chains in the modifications, the simulation results do support the experimentally observed effects of the length of the carbon chain on the duplex stability. We first monitored and

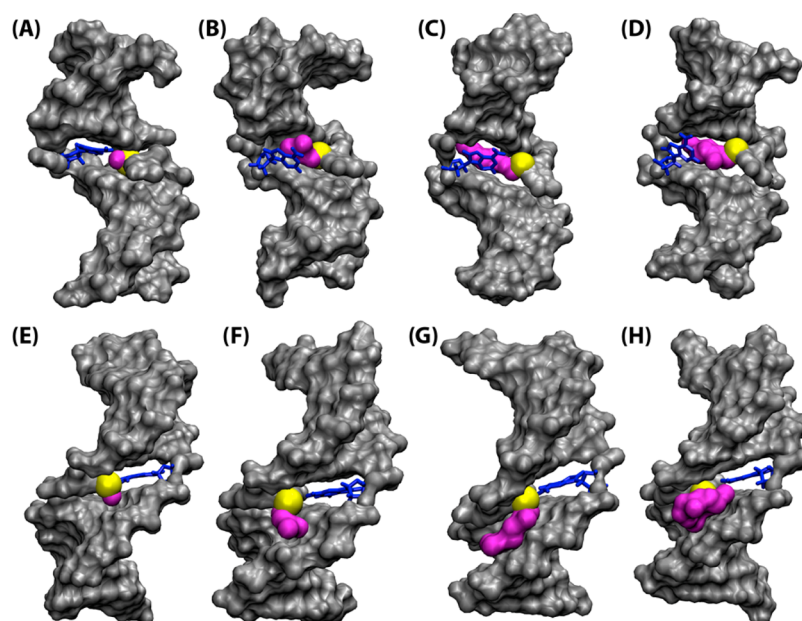


Figure 8. Representative snapshots from molecular dynamics simulations of 11-nt DNA duplexes containing xT:A (A–D) and xT:G (E–H). The duplex is shown in gray, the sulfur atom in yellow, and the hydrophobic chain of the modified group with different length in magenta (including methyl-, dimethylallyl-, geranyl-, and farnesyl-groups). The base paired to the (xT), either an A or G, is shown in blue sticks.

analyzed the base-pairing dynamics at the xT sites by measuring the distances between the positions of the C1' atom of the participating bases (xT-A/G). As shown in Figure 6B, the xT:A pairs (red line) exhibit a wide range of C1'–C1' distances, which increases with the length of carbon chain in the modifications. In contrast, all of the modified xT:G pairs (black line) are found to be stable with only small changes in the C1'–C1' distance.

The loss of stable base-pairing interactions also reduces stacking between bases, which further affects the duplex stability. We plotted the probability of observing different stacking distances between A or G (paired to xT) and their two neighboring bases (C on the 5' end and A on the 3' end). The stacking distance is calculated as the distance between the center of mass of the participating nucleobases. It was observed that duplexes with xT:A pairs experience destabilized stacking interactions, as reflected by the wider distribution of stacking distances (Figure 7A), although the stacking distance itself between A and its 5'-neighboring C does not change dramatically with the introduction of each terpene group. The stacking distance between A and its 3'-A residue is clearly higher when A is base paired with a modified T; and the longer the carbon chain, the larger the overall stacking distance, which is consistent with the steady drop in the melting temperatures for xT:A duplexes as a function of the length of the carbon chain (Figure 7B). In the case of duplexes with xT:G pair, however, the base pairing is still maintained by two stable hydrogen bonds. As a consequence of stable base pairing, the stacking interactions between G and its neighboring bases are also maintained regardless of the length of the modification. Interestingly, the observed stacking distance is longer at the 5'-end for the native thymidine when compared to those with the modifications (Figure 7C). This can be attributed to the difference in base-pairing conformations of the xT:G base pair in the presence and absence of the modifications. At the 3' end, the modified T does not alter the stacking distance between G and A (Figure 7D).

The study of base-pairing and base-stacking interactions provide structural insight into the experimentally observed duplex stability in case of xT:A-pair-containing duplexes. However, to further understand the enhanced stability introduced by the geranyl group in case of xT:G-pair-containing duplexes, dominant conformations adopted by the xT:(A/G) base pairs during the course of the simulation were analyzed (Figure 8). As shown in Figure 8A–D, as a result of the loss of stable base-pairing interactions of xT:A pair, the modified carbon chains in the duplex can swing into the core of the helical structure and push out the paired adenosine. The longer the chain length, the easier it is to push out the opposite A, dramatically disrupting the local structures and making the duplex more unstable. In the case of xT:G paired duplex, however, the overall helical structure at the site of the modification is maintained. The geranyl and farnesyl groups in this case, can fit into the DNA minor groove, which protects the neighboring base pairs and adds additional stability to the duplex. In contrast, the methyl or dimethylallyl groups are not long enough to offer such protection to the neighboring bases, as shown in Figure 8E–H. These observations collectively provide a plausible explanation for the significance of the length of the naturally occurring C-10 carbon chain at the 2-thio position and its ability to promote base-pairing stability and specificity of xT:G and xT:A pairs.

CONCLUSIONS

In conclusion, this work confirms that the geranyl group in the 2-thiouridine derivatives is the right size for promoting the recognition of G over A. Although all the substituents at the 2-thio position alter the protonation state of the N-3 atom changing it from being a hydrogen bond donor to a hydrogen bond acceptor, they affect the overall base-pairing stability and specificity in different fashions. Interestingly, our thermal stability study showed that the modified thymidine loses its base-pairing discrimination in the presence of short carbon chains like methyl (C-1) and dimethylallyl (C-5) groups. In

contrast, the longer farnesyl group (C-15 lengths of terpene chain) shows very similar effects to the overall duplex stability and base-pairing specificity when compared to the geranyl group. The molecular dynamic simulation studies suggested that, for the (xT):A pair, the modified terpene chain interrupts base pairing and widens the DNA duplex at the modified site, as the terpene chain grows longer, resulting in a constant decline in overall DNA duplex stability. In the case of xT:G-pair-containing duplexes, the long-chain terpenes can fit into the minor groove of DNA duplex and increase the duplex stability. This phenomenon could not be observed with the shorter carbon chains like the methyl and dimethylallyl groups. In our data set, the geranyl group (C-10) was the first carbon chain length, wherein base-pairing discrimination was observed. Although the farnesyl group shows comparable base-pairing specificity to the geranyl group, the ges^2T provides relatively higher stability to overall DNA duplexes than fas^2T does, and it is hypothesized to be a more economical way for cells to use geranyl group with less carbon atoms than farnesyl or other longer terpene groups in modifying the 2-thiouridine, which represents an evolutionary advantage of the geranyl group. Of course, the availability of building blocks in cells and a working enzyme to recognize these substrates are other two important factors to be considered to fully understand nature's unique selection of geranyl group in tRNA modification. Most likely, the farnesyl or other terpene pyrophosphates are not efficient substrates of SelU, the natural enzyme that installs geranyl group at 2-thiouridine residues in tRNAs.

MATERIALS AND METHODS

Synthesis of 2-Thio-geranyluridine Derivative Phosphoramidite. 5'-DMTr-2-Thiothymidine (Compound 9). The 2-thiothymidine **8** (500 mg, 1.95 mmol) was coevaporated with dry pyridine (5 mL) for three times to remove the potential water in the starting material **8**, which was subsequently redissolved in the pyridine (5 mL), followed by the slow addition of the pyridine solution of dimethoxytrityl chloride (760 mg, 2.25 mmol) at room temperature. The reaction mixture was kept stirring for 4 h before being quenched with anhydrous methanol (5.0 mL) and evaporated in vacuum. The residue was extracted by dichloromethane and water. The organic layer was washed with saturated sodium bicarbonate solution, dried over magnesium sulfate, filtered, and the solvent was removed in vacuum. The residue was purified by silica gel flash chromatography (eluent 1% methanol in CH_2Cl_2 containing 1% of Et_3N) to afford **9** as a white solid (922 mg, 85.2%). TLC R_f = 0.60 (1% MeOH in CH_2Cl_2 with 1% triethylamine). 1H NMR (400 MHz, $CDCl_3$) δ 7.89 (s, 1H), 7.69 (t, J = 7.84 Hz, 1H), 7.40 (t, J = 7.48 Hz, 2H), 7.30–7.26 (m, 4H), 7.23 (d, J = 7.16 Hz, 1H), 6.97 (t, J = 6.16 Hz, 1H), 6.83 (dd, J_1 = 8.88 Hz, J_2 = 1.72 Hz, 4H), 4.62–4.59 (m, 1H), 4.13 (d, J = 3.08 Hz, 1H), 3.77 (s, 6H), 3.55 (dd, J_1 = 10.92 Hz, J_2 = 2.72 Hz, 1H), 3.48 (dd, J_1 = 10.56 Hz, J_2 = 2.72 Hz, 1H), 2.68 (dd, J_1 = 14.36 Hz, J_2 = 2.65 Hz, 1H), 2.63 (dd, J_1 = 6.16 Hz, J_2 = 4.12 Hz, 1H), 2.33–2.26 (m, 1H), 1.45 (s, 3H); ^{13}C NMR (100 MHz, $CDCl_3$) δ 174.26, 161.41, 158.61, 149.34, 144.20, 136.43, 136.24, 135.27, 129.98, 128.02, 127.89, 127.05, 123.78, 116.22, 113.17, 89.79, 86.80, 86.56, 71.07, 62.92, 55.15, (45.56), 41.13, 12.04 (10.55); ESI-MS: $[M + Na]^+$: 583.1892 (calcd: 583.1879).³¹

S-Geranyl Analogues Modified 5'-DMTr-2-Thiothymidines (Compounds 10a–d). For the synthesis of compounds **10a–d**, the methanol solution containing **9** (200 mg, 0.36 mmol), N,N -diisopropylethylamine (260 μ L, 1.48 mmol) and the terpene bromides, for example, iodomethane (66.48 μ L, 1.08 mmol, for **10a**), 3,3-dimethylallyl bromide (82.26 μ L, 0.72 mmol, for **10b**), farnesyl bromide (170 μ L, 0.74 mmol, for **10c**), and farnesyl bromide (202.4 μ L, 0.68 mmol, for **10d**), respectively, was stirred at 25 °C for 12 h when the starting material was completely consumed. The resulting reaction mixture was quenched with water, washed with brine

(8 \times 10 mL), and dried over Na_2SO_4 . The crude product was concentrated in vacuum and directly subjected to a flash silica gel chromatography using CH_2Cl_2 containing 1% MeOH and 1% Et_3N as eluent. White solids with over 90% of isolated yield could be obtained for each of compound **10**.

10a. 1H NMR (400 MHz, $CDCl_3$) δ 7.83 (s, 1H), 7.52–7.14 (m, 9H), 6.86–6.75 (m, 4H), 6.21 (t, J = 6.0 Hz, 1H), 4.64 (m, 1H), 4.13 (m, 1H), 3.78 (s, 6H), 3.54 (dd, J_1 = 3.2 Hz, J_2 = 10.8 Hz, 1H), 3.41 (dd, J_1 = 2.8, J_2 = 10.8 Hz, 1H), 3.2 (s, 1H), 2.58 (s, 3H), 2.51–2.45 (m, 1H), 2.34–2.25 (m, 1H), 1.55 (s, 3H); ^{13}C NMR (100 MHz, $CDCl_3$) δ 169.94, 161.08, 159.04, 144.478, 135.58, 135.52, 134.76, 130.32, 128.36, 128.27, 127.44, 119.28, 113.57, 88.30, 87.35, 87.02, 72.31, 63.58, 55.50, 41.96, 14.95, 13.57; ESI-MS $[M]^+$: 574.0396 (calcd MS: 574.2138)

10b. 1H NMR (400 MHz, $CDCl_3$) δ 7.77 (s, 1H), 7.40–7.23 (m, 9H), 6.84–6.82 (m, 4H), 6.23 (t, J = 4.0 Hz, 1H), 5.32–5.22 (m, 1H), 4.61 (m, 1H), 4.35–4.25 (m, 1H), 4.21–4.13 (m, 1H), 4.09–4.11 (m, 1H), 3.85–3.95 (m, 2H), 3.78 (s, 6H), 3.50 (dd, J_1 = 3.2 Hz, J_2 = 10.8 Hz, 1H), 3.39 (dd, J_1 = 2.8, J_2 = 10.8 Hz, 1H), 2.80 (s, 1H), 2.51–2.40 (m, 1H), 2.35–2.28 (m, 1H), 1.72 (s, 3H), 1.71 (s, 3H), 1.55 (s, 3H); ^{13}C NMR (100 MHz, $CDCl_3$) δ 169.89, 160.84, 158.58, 144.25, 138.82, 135.13, 135.04, 130.00, 128.05, 126.99, 118.72, 116.73, 113.16, 88.34, 86.83, 74.35, 72.28, 69.04, 62.18, 55.11, 45.92, 41.81, 34.01, 29.37, 25.61, 17.89, 13.97, 13.13; ESI-MS: $[M + H]^+$: 629.2643 (calcd MS: 629.2607).

10c. 1H NMR (400 MHz, $CDCl_3$) δ 7.80 (s, 1H), 7.39 (d, J = 7.16 Hz, 2H), 7.30–7.16 (m, 6H), 6.83 (s, 2H), 6.81 (s, 2H), 6.24 (t, J = 5.80 Hz, 1H), 5.31 (t, J = 7.88 Hz, 1H), 5.06 (t, J = 7.88 Hz, 1H), 4.64 (t, J = 3.08 Hz, 1H), 4.12 (d, J = 2.72 Hz, 1H), 3.96–3.86 (m, 2H), 3.77 (s, 6H), 3.50 (dd, J_1 = 10.60 Hz, J_2 = 3.08 Hz, 1H), 3.41–3.37 (m, 1H), 2.51–2.46 (m, 1H), 2.37–2.30 (m, 1H), 2.10–2.00 (m, 5H), 1.70 (s, 3H), 1.67 (s, 3H), 1.59 (s, 3H), 1.52 (s, 3H); ^{13}C NMR (100 MHz, $CDCl_3$) δ 169.59, 160.71, 158.63, 144.12, 142.58, 135.22, 134.43, 131.68, 129.96, 129.02, 127.99, 127.90, 127.70 (127.65), 127.06, 126.65, 123.64, 118.93, 116.32, 113.19, 113.04 (113.00), 105.43, 87.95, 86.93, 86.67, 71.90, 63.23, 55.13, 41.62, 39.46, 30.67, 26.26, 25.58, 17.61, 16.26, 13.27; ESI-MS: $[M + H]^+$: 697.3341 (calcd MS: 697.3311).

10d. 1H NMR (400 MHz, $CDCl_3$) δ 7.82 (s, 1H), 7.38–7.18 (m, 9H), 6.80–6.78 (m, 4H), 6.22 (t, J = 4.0 Hz, 1H), 5.34–5.06 (m, 3H), 4.64 (m, 1H), 4.15–4.11 (m, 1H), 3.92–3.86 (m, 2H), 3.74 (s, 6H), 3.48–3.45 (dd, J_1 = 3.2 Hz, J_2 = 10.8 Hz, 1H), 3.38–3.36 (dd, J_1 = 3.2, J_2 = 10.8 Hz, 1H), 2.50–2.30 (m, 2H), 2.06–2.01 (m, 8H), 1.68 (s, 3H), 1.65 (s, 3H), 1.57 (s, 6H), 1.47 (s, 3H); ^{13}C NMR (100 MHz, $CDCl_3$) δ 170.93, 160.85, 158.65, 144.23, 142.10, 140.38, 135.33, 135.22, 131.20, 130.02, 128.07, 124.29, 123.56, 118.85, 113.20, 88.18, 86.91, 74.40, 69.06, 62.22, 57.62, 55.13, 49.90, 45.86, 41.75, 39.62, 33.58, 31.67, 29.34, 25.64, 22.51, 21.22, 17.63, 16.33, 14.05, 13.24; ESI-MS: $[M + H]^+$: 765.3902 (calcd MS: 765.3859).

S-Geranyl Analogues Modified 5'-DMTr-2-Thiothymidine Phosphoramidites (Compounds 11a–d). For the synthesis of compounds **11a–d**, the solution of compound **10** (200 mg), N,N -diisopropylethylamine (DIPEA) (2 equiv) in anhydrous CH_2Cl_2 (5.0 mL), and 2-cyanoethyl N,N -diisopropylchlorophosphoramidite (1.5 equiv) was stirred at RT for 5 h under Ar protection. The resulting reaction mixture with the two diastereomers was concentrated in vacuum and directly subjected to silica gel flash chromatography using CH_2Cl_2 containing 0.5% MeOH and 1% Et_3N as eluent to give **11** as a light yellowish sticky liquid with yields ~75–80%. The compounds were characterized by ^{31}P NMR and ESI-MS. **11a.** ^{31}P NMR ($CDCl_3$) δ 149.84, 149.22; ESI-MS: $[M + H]^+$: 776.5565 (calcd MS: 776.3216). **11b.** ^{31}P NMR ($CDCl_3$) δ 149.16, 148.72; ESI-MS: $[M + H]^+$: 829.3734 (calcd MS: 829.3686). **11c.** ^{31}P NMR ($CDCl_3$) δ 149.16, 148.77; ESI-MS: $[M + H]^+$: 897.4419 (calcd MS: 897.4390). **11d.** ^{31}P NMR ($CDCl_3$) δ 149.10, 148.62; ESI-MS: $[M + H]^+$: 965.5061 (calcd MS: 965.4938).

Synthesis of DNA Oligonucleotides. The DNA oligonucleotides were chemically synthesized at 1.0 μ mol scales by solid-phase synthesis using an Oligo-800 DNA synthesizer. The system was protected with helium gas. All the reagents were purchased from ChemGenes. The

synthesis was carried out on control-pore glass (CPG-500) with succinate linking to the first trityl protected nucleoside at the 3' end. After the trityl group was removed by 3% trichloroacetic acid in dichloromethane, the next phosphoramidite (0.05 M) was activated and incorporated using 0.25 M 5-ethylthio tetrazole in acetonitrile. Acetic anhydride and *n*-methylimidazole in tetrahydrofuran and pyridine were used for capping. The oxidation was performed using iodine in pyridine/H₂O/THF. The modified phosphoramidite was dissolved in dichloromethane and at the concentration of 0.1 M. The DNA oligonucleotides were synthesized with DMTr-on form. The oligonucleotide-CPG was cleaved and the phosphate backbone was deprotected using concentrated ammonium hydroxide solution at RT for overnight. The samples were concentrated using speed-vac prior to the purification.

DNA Oligonucleotides Purification. After the cleavage step, the DNA oligonucleotides were directly purified by reverse-phase HPLC. The Ultimate XB-C18 column from Welch, 10 μ m spherical packing, and 21.2 \times 250 mm in size was used with the flow rate of 6 mL/min. The buffer A was 20 mM TEAAc (triethylammonium acetate, pH 7.1) buffer, and the buffer B was 50% of 20 mM TEAAc in acetonitrile. The undesired short strand was separated and eluted out with gradient mode of 5–100% over 20 min. The 5' trityl protecting oligonucleotides was eluted at 100% of buffer B. After lyophilizing, the oligonucleotides were detritylated by 3% TCA in water and desalted with Waters Sep-Pak C18 cartridge.

Thermodenaturation Studies of DNA Duplexes. Equal amounts of the purified DNA with the modified strand and its native complementary strand with matched and mismatched bases opposite to the modified nucleotide were mixed. The mixtures were diluted to a final concentration of 1.5 μ M in 10 mM sodium phosphate buffer containing 100 mM sodium chloride (pH 6.5). The solutions were heated to 95 $^{\circ}$ C for 5 min and slowly cooled to RT at the rate of 1 $^{\circ}$ C/min. The solutions were subsequently stored at 4 $^{\circ}$ C for overnight prior the UV-melting temperature experiment. The Cary-300 UV-visible spectrometer equipped with a temperature controller system was used for the UV-melting studies. Prior to thermal denaturation, the duplex solutions were bubbled with argon for 5 min. The absorption was acquired at 260 nm with temperature control by heating from 5 to 85 $^{\circ}$ C and cooling from 85 to 5 $^{\circ}$ C at the rate of 0.5 $^{\circ}$ C/min. All the data were collected with 4 ramps. The thermodynamic parameters of each duplex were obtained by fitting the melting curves using the MeltWin 3.5 program.⁴²

Computational Methods. To study the modifications in the context of the duplex in MD simulations, we obtained AMBER⁴³ type force-field parameters for the modified nucleotides. For obtaining the partial charges on atoms, we used the online RESP/ESP charge-fitting server, REDS.⁴⁴ The geometry of the modified nucleoside was energy minimized at Hartree–Fock level theory and 6-31G* basis-sets were employed to arrive at a set of partial charges.⁴⁵ AMBER-99 force-field parameters were used for bonded interactions⁴³ and AMBER-99 parameters with Chen–Garcia corrections were used for LJ interactions.⁴⁶ The unmodified DNA duplex 5'-CTTCTXGTCCG-3' and 3'-GAAGAYCAGGC-5' consistent with experimental work presented here, was constructed in B-form using Nucleic Acid Builder (NAB) suite of AMBER 11 package. X and Y correspond to xT (modified thymidine) and A/C/G/T respectively. Mutations going from A \rightarrow G(G,C,T) were introduced using MOE.⁴⁷ The modifications were incorporated by overlapping the modified nucleotide (xT) over the canonical one and then replacing the canonical T.

Molecular dynamic simulations were performed using GROMACS-5.0.7 package.⁴⁸ The simulation system included the DNA duplex in a solution of 1 M NaCl solution in a 3D periodic box. The box size was 6 \times 6 \times 6 nm³ containing the DNA duplex, Na⁺ ions and Cl⁻ ions and water molecules. Each system was subjected to energy minimization to prevent any overlap of atoms followed by a 10 ns equilibration MD run. Five parallel simulations with the same equilibrated starting conformations but with different starting velocities were performed for 100 ns each, totaling 0.5 μ s of production run in each case. The MD simulations incorporated leapfrog algorithm with a 2 fs time-step to integrate the equations of motion. The system was maintained at 300

K using the velocity rescaling thermostat.⁴⁹ The pressure was maintained at 1 bar using Berendsen⁵⁰ and Parrinello–Rahman barostat⁵¹ for equilibration and production, respectively. The long-range electrostatic interactions were calculated using particle mesh Ewald (PME)⁵² algorithm with a real space cutoff of 1.2 nm. LJ interactions were also truncated at 1.2 nm. The TIP3P model⁵³ was used to represent the water molecules, and the LINCS algorithm⁵⁴ was used to constrain the motion of hydrogen atoms bonded to heavy atoms. Coordinates of the DNA duplex were stored every 1 ps for further analysis.

■ ASSOCIATED CONTENT

Supporting Information

The Supporting Information is available free of charge on the ACS Publications website at DOI: 10.1021/acscchembio.7b00108.

ESI-MS spectra of intermediates 10a–d and 11a–d; MS of modified oligonucleotides (PDF)

■ AUTHOR INFORMATION

Corresponding Author

*E-mail: jsheng@albany.edu.

ORCID

Alan Chen: 0000-0001-8246-2935

Jia Sheng: 0000-0001-6198-390X

Author Contributions

#(P.H. and S.V.) These authors contribute equally to this work.

Notes

The authors declare no competing financial interest.

■ ACKNOWLEDGMENTS

This work is supported by the start-up fund from University at Albany, State University of New York. R.W. was supported by postdoctoral fellowship from Simons Foundation (338863, R.W.) during this work. We thank L. Seebald for her help in mass-spectrometry analyses.

■ REFERENCES

- (1) Machnicka, M. A., Milanowska, K., Osman Oglou, O., Purta, E., Kurkowska, M., Olchowik, A., Januszewski, W., Kalinowski, S., Dunin-Horkawicz, S., Rother, K. M., Helm, M., Bujnicki, J. M., and Grosjean, H. (2013) MODOMICS: a database of RNA modification pathways–2013 update. *Nucleic Acids Res.* 41, D262–267.
- (2) Cantara, W. A., Crain, P. F., Rozenski, J., McCloskey, J. A., Harris, K. A., Zhang, X., Vendeix, F. A., Fabris, D., and Agris, P. F. (2011) The RNA Modification Database, RNAMDB: 2011 update. *Nucleic Acids Res.* 39, D195–201.
- (3) Nachtergaele, S., and He, C. (2017) The emerging biology of RNA post-transcriptional modifications. *RNA Biol.* 14, 156.
- (4) Sample, P. J., Koreny, L., Paris, Z., Gaston, K. W., Rubio, M. A., Fleming, I. M., Hinger, S., Horakova, E., Limbach, P. A., Lukes, J., and Alfonzo, J. D. (2015) A common tRNA modification at an unusual location: the discovery of wycosine biosynthesis in mitochondria. *Nucleic Acids Res.* 43, 4262–4273.
- (5) Phizicky, E. M., and Hopper, A. K. (2010) tRNA biology charges to the front. *Genes Dev.* 24, 1832–1860.
- (6) Hopper, A. K., and Shaheen, H. H. (2008) A decade of surprises for tRNA nuclear-cytoplasmic dynamics. *Trends Cell Biol.* 18, 98–104.
- (7) Liu, N., Dai, Q., Zheng, G., He, C., Parisien, M., and Pan, T. (2015) N(6)-methyladenosine-dependent RNA structural switches regulate RNA-protein interactions. *Nature* 518, 560–564.
- (8) Endres, L., Dedon, P. C., and Begley, T. J. (2015) Codon-biased translation can be regulated by wobble-base tRNA modification systems during cellular stress responses. *RNA Biol.* 12, 603–614.

- (9) Huang, H. Y., and Hopper, A. K. (2016) Multiple Layers of Stress-Induced Regulation in tRNA Biology. *Life (Basel, Switz.)* 6, 16.
- (10) Liu, F., Clark, W., Luo, G., Wang, X., Fu, Y., Wei, J., Wang, X., Hao, Z., Dai, Q., Zheng, G., Ma, H., Han, D., Evans, M., Klungland, A., Pan, T., and He, C. (2016) ALKBH1-Mediated tRNA Demethylation Regulates Translation. *Cell* 167, 816.
- (11) Joyce, G. F. (2002) The antiquity of RNA-based evolution. *Nature* 418, 214–221.
- (12) Iben, J. R., and Maraia, R. J. (2012) tRNAomics: tRNA gene copy number variation and codon use provide bioinformatic evidence of a new anticodon:codon wobble pair in a eukaryote. *RNA* 18, 1358–1372.
- (13) Graham, W. D., Barley-Maloney, L., Stark, C. J., Kaur, A., Stolyarchuk, C., Sproat, B., Leszczynska, G., Malkiewicz, A., Safwat, N., Mucha, P., Guenther, R., and Agris, P. F. (2011) Functional recognition of the modified human tRNA^{Lys}3(UUU) anticodon domain by HIV's nucleocapsid protein and a peptide mimic. *J. Mol. Biol.* 410, 698–715.
- (14) Bilbille, Y., Gustilo, E. M., Harris, K. A., Jones, C. N., Lusic, H., Kaiser, R. J., Delaney, M. O., Spremulli, L. L., Deiters, A., and Agris, P. F. (2011) The human mitochondrial tRNA^{Met}: structure/function relationship of a unique modification in the decoding of unconventional codons. *J. Mol. Biol.* 406, 257–274.
- (15) Sheppard, K., Akochy, P. M., and Soll, D. (2008) Assays for transfer RNA-dependent amino acid biosynthesis. *Methods* 44, 139–145.
- (16) Sanders, C. L., Lohr, K. J., Gambill, H. L., Curran, R. B., and Curran, J. F. (2008) Anticodon loop mutations perturb reading frame maintenance by the E site tRNA. *RNA* 14, 1874–1881.
- (17) Zhou, X.-L., Ruan, Z.-R., Wang, M., Fang, Z.-P., Wang, Y., Chen, Y., Liu, R.-J., Eriani, G., and Wang, E.-D. (2014) A minimalist mitochondrial threonyl-tRNA synthetase exhibits tRNA-isoacceptor specificity during proofreading. *Nucleic Acids Res.* 42, 13873–13886.
- (18) Hopper, A. K. (2013) Transfer RNA post-transcriptional processing, turnover, and subcellular dynamics in the yeast *Saccharomyces cerevisiae*. *Genetics* 194, 43–67.
- (19) Shepherd, J., and Ibba, M. (2013) Direction of aminoacylated transfer RNAs into antibiotic synthesis and peptidoglycan-mediated antibiotic resistance. *FEBS Lett.* 587, 2895–2904.
- (20) Laxman, S., Sutter, B. M., Wu, X., Kumar, S., Guo, X., Trudgian, D. C., Mirzaei, H., and Tu, B. P. (2013) Sulfur amino acids regulate translational capacity and metabolic homeostasis through modulation of tRNA thiolation. *Cell* 154, 416–429.
- (21) Murphy, F. V. t., Ramakrishnan, V., Malkiewicz, A., and Agris, P. F. (2004) The role of modifications in codon discrimination by tRNA(Lys)UUU. *Nat. Struct. Mol. Biol.* 11, 1186–1191.
- (22) Motorin, Y., Lyko, F., and Helm, M. (2010) 5-methylcytosine in RNA: detection, enzymatic formation and biological functions. *Nucleic Acids Res.* 38, 1415–1430.
- (23) Armengod, M. E., Moukadiri, I., Prado, S., Ruiz-Partida, R., Benitez-Paez, A., Villarroja, M., Lomas, R., Garzon, M. J., Martinez-Zamora, A., Meseguer, S., and Navarro-Gonzalez, C. (2012) Enzymology of tRNA modification in the bacterial MnmEG pathway. *Biochimie* 94, 1510–1520.
- (24) Ashraf, S. S., Sochacka, E., Cain, R., Guenther, R., Malkiewicz, A., and Agris, P. F. (1999) Single atom modification (O→S) of tRNA confers ribosome binding. *RNA* 5, 188–194.
- (25) Yarian, C., Marszalek, M., Sochacka, E., Malkiewicz, A., Guenther, R., Miskiewicz, A., and Agris, P. F. (2000) Modified nucleoside dependent Watson-Crick and wobble codon binding by tRNA^{Lys}UUU species. *Biochemistry* 39, 13390–13395.
- (26) Kruger, M. K., Pedersen, S., Hagervall, T. G., and Sorensen, M. A. (1998) The modification of the wobble base of tRNA^{Glu} modulates the translation rate of glutamic acid codons in vivo. *J. Mol. Biol.* 284, 621–631.
- (27) Yarian, C., Townsend, H., Czestkowski, W., Sochacka, E., Malkiewicz, A. J., Guenther, R., Miskiewicz, A., and Agris, P. F. (2002) Accurate translation of the genetic code depends on tRNA modified nucleosides. *J. Biol. Chem.* 277, 16391–16395.
- (28) Wolfe, M. D., Ahmed, F., Lacourciere, G. M., Lauhon, C. T., Stadtman, T. C., and Larson, T. J. (2004) Functional diversity of the rhodanese homology domain: the *Escherichia coli* ybbB gene encodes a selenophosphate-dependent tRNA 2-selenouridine synthase. *J. Biol. Chem.* 279, 1801–1809.
- (29) Dumelin, C. E., Chen, Y., Leconte, A. M., Chen, Y. G., and Liu, D. R. (2012) Discovery and biological characterization of geranylated RNA in bacteria. *Nat. Chem. Biol.* 8, 913–919.
- (30) Chen, P., Crain, P. F., Nasvall, S. J., Pomerantz, S. C., and Bjork, G. R. (2005) A "gain of function" mutation in a protein mediates production of novel modified nucleosides. *EMBO J.* 24, 1842–1851.
- (31) Wang, R., Vangaveti, S., Ranganathan, S. V., Basanta-Sanchez, M., Haruehanroengra, P., Chen, A., and Sheng, J. (2016) Synthesis, base pairing and structure studies of geranylated RNA. *Nucleic Acids Res.* 44, 6036–6045.
- (32) Wang, R., Ranganathan, S. V., Basanta-Sanchez, M., Shen, F., Chen, A., and Sheng, J. (2015) Synthesis and base pairing studies of geranylated 2-thiothymidine, a natural variant of thymidine. *Chem. Commun.* 51, 16369–16372.
- (33) Sierant, M., Leszczynska, G., Sadowska, K., Dziergowska, A., Rozanski, M., Sochacka, E., and Nawrot, B. (2016) S-Geranyl-2-thiouridine wobble nucleosides of bacterial tRNAs; chemical and enzymatic synthesis of S-geranylated-RNAs and their physicochemical characterization. *Nucleic Acids Res.* 44, 10986–10998.
- (34) Cane, D. E., and Ikeda, H. (2012) Exploration and mining of the bacterial terpenome. *Acc. Chem. Res.* 45, 463–472.
- (35) Mori, T., Zhang, L., Awakawa, T., Hoshino, S., Okada, M., Morita, H., and Abe, I. (2016) Manipulation of prenylation reactions by structure-based engineering of bacterial indolactam prenyltransferases. *Nat. Commun.* 7, 10849.
- (36) Bartos, P., Maciaszek, A., Rosinska, A., Sochacka, E., and Nawrot, B. (2014) Transformation of a wobble 2-thiouridine to 2-selenouridine via S-geranyl-2-thiouridine as a possible cellular pathway. *Bioorg. Chem.* 56, 49–53.
- (37) Jager, G., Chen, P., and Bjork, G. R. (2016) Transfer RNA Bound to MnmH Protein Is Enriched with Geranylated tRNA—A Possible Intermediate in Its Selenation? *PLoS One* 11, e0153488.
- (38) Sun, H., Sheng, J., Hassan, A. E., Jiang, S., Gan, J., and Huang, Z. (2012) Novel RNA base pair with higher specificity using single selenium atom. *Nucleic Acids Res.* 40, 5171–5179.
- (39) Hassan, A. E., Sheng, J., Zhang, W., and Huang, Z. (2010) High fidelity of base pairing by 2-selenothymidine in DNA. *J. Am. Chem. Soc.* 132, 2120–2121.
- (40) Scott, A. I. (1997) How were porphyrins and lipids synthesized in the RNA world? *Tetrahedron Lett.* 38, 4961–4964.
- (41) Sintim, H. O., and Kool, E. T. (2006) Enhanced base pairing and replication efficiency of thiothymidines, expanded-size variants of thymidine. *J. Am. Chem. Soc.* 128, 396–397.
- (42) McDowell, J. A., and Turner, D. H. (1996) Investigation of the structural basis for thermodynamic stabilities of tandem GU mismatches: solution structure of (rGAGGUCUC)₂ by two-dimensional NMR and simulated annealing. *Biochemistry* 35, 14077–14089.
- (43) Cornell, W. D., Cieplak, P., Bayly, C. L., Gould, I. R., Merz, K. M., Ferguson, D. M., Spellmeyer, D. C., Fox, T., Caldwell, J. W., and Kollman, P. A. (1995) A Second Generation Force Field for the Simulation of Proteins, Nucleic Acids, and Organic Molecules. *J. Am. Chem. Soc.* 117, 5179–5197.
- (44) Dupradeau, F. Y., Pigache, A., Zaffran, T., Savineau, C., Lelong, R., Grivel, N., Lelong, D., Rosanski, W., and Cieplak, P. (2010) The R.E.D. tools: advances in RESP and ESP charge derivation and force field library building. *Phys. Chem. Chem. Phys.* 12, 7821–7839.
- (45) Cornell, W. D., Cieplak, P., Bayly, C. L., and Kollman, P. A. (1993) Application of RESP charges to calculate conformational energies, hydrogen bond energies, and free energies of solvation. *J. Am. Chem. Soc.* 115, 9620–9631.
- (46) Chen, A. A., and Garcia, A. E. (2013) High-resolution reversible folding of hyperstable RNA tetraloops using molecular dynamics simulations. *Proc. Natl. Acad. Sci. U. S. A.* 110, 16820–16825.

(47) Chemical Computing Group, Inc. (CCG, Inc.) (2016) *Molecular Operating Environment (MOE)*, CCG, Inc., Montreal, QC, Canada.

(48) Hess, B., Kutzner, C., van der Spoel, D., and Lindahl, E. (2008) GROMACS 4: Algorithms for Highly Efficient, Load-Balanced, and Scalable Molecular Simulation. *J. Chem. Theory Comput.* 4, 435–447.

(49) Bussi, G., Donadio, D., and Parrinello, M. (2007) Canonical sampling through velocity rescaling. *J. Chem. Phys.* 126, 014101.

(50) Berendsen, H. J. C. P., Postma, J. P. M., van Gunsteren, W. F., DiNola, A., and Haak, J. R. (1984) Molecular dynamics with coupling to an external bath. *J. Chem. Phys.* 81, 3684–3690.

(51) Parrinello, M., and Rahman, A. (1981) Polymorphic transitions in single crystals: A new molecular dynamics method. *J. Appl. Phys.* 52, 7182–7190.

(52) Darden, T., York, D., and Pedersen, L. (1993) Particle Mesh Ewald-an N.Log(N) method for Ewald sums in large systems. *J. Chem. Phys.* 98, 10089–10092.

(53) Jorgensen, W. L., Chandrasekhar, J., Madura, J. D., Impey, R. W., and Klein, M. L. (1983) Comparison of simple potential functions for simulating liquid water. *J. Chem. Phys.* 79, 926–935.

(54) Hess, B., Bekker, H., Berendsen, H. J. C., and Fraaije, J. G. E. M. (1997) LINCS: A linear constraint solver for molecular simulations. *J. Comput. Chem.* 18, 1463–1472.